

*Received October 11, 2013; reviewed; accepted December 31, 2013*

## **SURFACE PROBABILITY MODEL FOR ESTIMATION OF SIZE DISTRIBUTION ON A CONVEYOR BELT**

**Zelin ZHANG, Jianguo YANG, Dongyang Dou**

National Engineering Research Center of Coal Preparation and Purification, China University of Mining and Technology, Xuzhou, Jiangsu 221116, China; zhangzelin3180@163.com; scetyjg@126.com.

**Abstract:** Estimation of size distribution by image analysis is a key issue in mineral engineering. However, only the surface information of ore piles can be captured, which is a headache problem in this field while only a few researchers pay attention to this problem. A new surface probability model was proposed for estimation of size distribution on a conveyor belt based on the Chavez Model in this investigation. This model was tested and verified to have smaller errors in single size fraction but have bigger errors in multiple size fractions. Several error trends were found and a correction factor was introduced to correct the higher errors. A series of linear equations were developed to calculate this specific correction factor according to  $D_m$  (average particle size) and the height of pile. Therefore, empirical probability can be estimated by the specific correction factor and calculated probability, and the surface information of ore piles can be converted into the global information of piles.

**Keywords:** *size distribution; surface probability model; conveyor belt; particles*

### **Introduction**

Image analysis techniques have been used in mineral engineering since 1980. The related fields include the size distribution estimation (Al-Thyabat and Miles, 2006; Al-Thyabat et al., 2007; Casali et al., 2001; Chavez et al., 1996; Ko and Shang, 2011; King, 1982; Kemenny et al., 2001; Guyot et al., 2004; Zhao, 2013; Vallebuna et al., 2003; Zhang et al., 2012; Yang et al., 2013), ores grade estimation (Claudio et al., 2011; Jayson et al., 2007; Chatterjee et al., 2010a; Chatterjee et al., 2010b), ores type prediction (Perez et al., 1999; Singh and Rao, 2006; Tessier et al., 2007; Singh et al., 2010), and other related researches (Petruk, 1988a; Petruk, 1988b; Petruk, 1989; Petruk et al., 1991; Sun and Su, 2013). Among these fields, the estimation of size distribution is mostly studied and widely applied, such as blasting, crusher controlling and mineral processing.

The traditional measure of size distribution of ores is obtained by screening or sieving, which is considered to be accuracy but time-consuming, not suitable for real-time monitoring. Therefore, image analysis techniques have been used to estimate the size distribution. However, this method can only obtain the surface information of ore piles, which is a headache problem in this field and few researchers pay attention to this problem.

Chavez et al. proposed a model to estimate the probability of particles appearing on the surface of ores piles, shown in Eq. (1) (Chavez et al., 1996). This surface probability model is suitable for particles in a recipient with a constant height. They selected a typical modeling unit, like Fig. 1, and indicated a particle  $F_i$  of size  $D_i$  appearing on the surface depends on the number of particles within the height  $H$  of the unit. They stated that “the probability  $P_i$  within a given pile depends on the particle size, and that all particles of size  $i$  will have the same probability to appear on the surface”. In Eq. (1), given the average fragment size  $D_M$ , the expression  $(H - D_i)$  is the remaining height of the pile below the surface particle  $F_i$ , and  $(H - D_i) / D_M$  approximates the average number of particles within the remaining height. Therefore, the expression  $1 + (H - D_i) / D_M$  is the number of particles within the height  $H$  of unit, and the reciprocal is the probability of particle  $F_i$  of size  $D_i$  to appear on the surface. In Eq. (2),  $N_i$  is the sum of particles of size  $D_i$ , therefore  $E_i$  is the number of particles of size  $D_i$  on the surface.

$$P_i = \frac{1}{1 + (H - D_i) / D_M} \quad (1)$$

$$E_i = N_i P_i \quad (2)$$

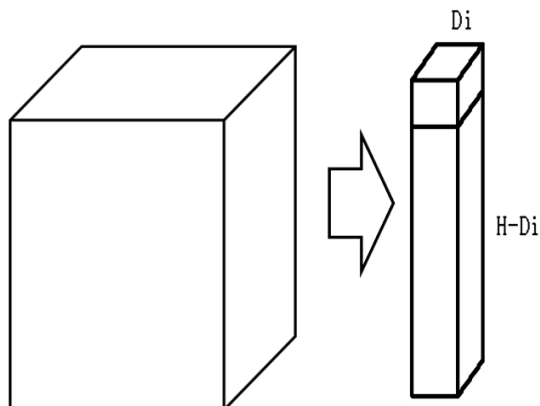


Fig. 1. Recipient with a constant height and the modeling unit

Chavez et al. tested the model using various recipients with different heights, such as 40 mm, 90 mm, 140 mm and 420 mm, and the results indicated the higher the pile

height is, the lower the error between empirical probability and calculated probability is. In addition, they indicated smaller block positions may not be modeled by simple geometric stacking, especially when much larger blocks were present within the pile. Although they found several error trends and concluded several reasons, the method of correction was not considered. They even stated the model is suitable for the piles on the truck or some recipients, but it is not suitable for the conveyor belt with non-uniform heights (Chavez et al., 1996).

A new surface probability model was proposed for the estimation of particles size distribution on a conveyor belt based on Chavez Model. Experiments have been carried out to test and verify the surface probability model in this investigation. Several error trends were concluded and a correction method proposed for errors between empirical probability and calculated probability also was introduced for multiple size fractions, which is a key finding for the correction of size distribution estimation on conveyor belt by image analysis techniques.

### Surface probability model for conveyor belt

Fig. 2(a) is a sketch map of conveyor belt, the maximum height and breadth of which are  $H$  and  $L$  respectively, and the length is random. The conveyor belt was divided into two same parts, which have the same surface probability in theory. Therefore, one of the divided parts was considered as the typical model unit of conveyor belt. However, this typical model unit also is a recipient with non-uniform heights. Then it continued to be divided into several sub-units by the interval of  $D_i$ , the heights of which can be considered as constant. Now each sub-unit is suitable for the probability model of Chavez, like Fig. 2(c).

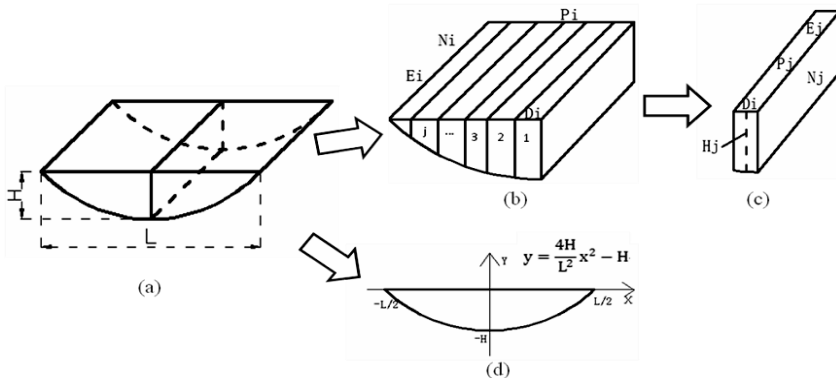


Fig. 2. Sketch map of typical model unit of conveyor belt and the parabola equation

In Fig. 2(b),  $i$  stands for size fraction;  $D_i$  is the mid-value of size fraction  $i$ ;  $N_i$  is the sum of particles in size fraction  $i$ ;  $E_i$  is the sum of surface particles in size fraction  $i$ ;  $P_i$  is the surface probability of particles in size fraction  $i$ ;  $j$  stands for sub-unit.

In Fig. 2(c),  $P_j$  is the surface probability of particles appearing on the sub-unit by Chavez Model, like Eq. (3), however, when  $H_j$  is less than  $D_i$ , the particles in size fraction  $i$  were considered as no chance to appear on the sub-unit, so the corresponding  $P_j$  is considered as zero. Supposing the particles of each size fraction were the uniform distribution, then  $N_j$  can be estimated by Eq. (4), then the surface particles of each sub-unit can be calculated by Eq. (5).

For the height  $H_j$  of each sub-unit, the profile of conveyor belt can be considered as a parabola, like Fig. 2(d). The equation of parabola can be developed by  $H$  and  $L$ . To test and verify the parabola equation, three lengths corresponding to three heights were measured by ruler and calculated by parabola equation, respectively, then the errors between measure and calculation is less than 3mm, so the parabola equation is considered to be able to calculate the height of sub-unit. Therefore,  $H_j$  was calculated by Eq. (6), and the horizontal ordinate was the mid-value of each sub-unit.

Finally,  $E_i$  is the sum of  $E_j$ , therefore  $P_i$  can be calculated by Eq. (7), which is the new surface probability model suitable for the conveyor belt and it only related with  $H_j$  and  $P_j$  at last.

$$P_j = \frac{1}{1 + (H_j - D_i) / D_M}, \text{ if } H_j < D_i, \quad P_j = 0 \tag{3}$$

$$N_j = \frac{H_j N_i}{\sum H_j} \tag{4}$$

$$E_j = N_j P_j \tag{5}$$

$$H_j = \left| \frac{4H}{L^2} x^2 - H \right|, \quad \frac{(2j-1)D_i}{2} x = \frac{D_i}{2}, \quad \frac{3D_i}{2} \tag{6}$$

$$P_i = \frac{E_i}{N_i} = \frac{\sum E_j}{N_i} = \frac{\sum N_j P_j}{N_i} = \frac{\sum H_j P_j}{\sum H_j} \tag{7}$$

**Model validation and test**

Surface probability model for conveyor belt was established and several experiments were carried out to test and validation the model and try to find out several relationships between empirical probability and calculated probability.

Fig. 3(a) and 3(b) are the equipments designed for testing surface probability model. A belt was closed by two organic glasses in two sides, which was convenient to measure the height and breadth of particle pile by tape, like Fig. 3(c). In addition, a mobile dam-board was used to adjust the height of particle pile, like Fig. 3(d).



Fig. 3. Equipment for testing the surface probability model

Model validation was carried out in four size fractions, 3–6 mm, 6–13 mm, 13–25 mm and 25–50 mm. The experimental procedures were as follows:

1. Counting the number of particles in each size fraction;
2. Mixing particle pile homogeneously on a flat tablet by rolling-over them from one place to another place three times;
3. Pouring the homogeneous pile into the belt, and using the mobile dam-board to control the height of pile;
4. Flattening the surface of pile and capturing the image of pile surface;
5. Counting the number of particles in each size fraction by drawing tool in computer, zoom functions in which was used to recognize the small particles on surface and marker function was used to count with no repetition.
6. The number of particles on surface divided by sum of particles in each size fraction was the empirical surface probability.
7. Repeating (2) to (6) three times, and considering the mean value of three empirical probabilities as the final empirical probability.
8. Calculating the surface probability of each size fraction by Eq. (7), and comparing the empirical probability and calculated probability.

**Test one:** particles in single size fraction were used to test the model in three heights of pile (100 mm, 120 mm and 150 mm).

The reason of selecting these three heights was that the height of conveyor belt on mineral industry was usually about 160 mm, therefore the heights of piles in belt usually were less than 160mm, but not more. In this test, the sums of each size fraction were 45833 particles in 3–6 mm, 4058 particles in 6–13 mm, 1250 particles in 13–25 mm and 262 particles in 25–50 mm. The breadths (B) corresponding to heights 100 mm, 120 mm and 150 mm were 434 mm, 476 mm and 532 mm, respectively. The values of  $D_m$  of four size fractions were 4.5 mm, 9.5 mm, 19.5 mm and 37.5 mm, respectively. Fig. 4(a) is the images of four size fractions captured in the height of 100 mm, and the expression “3–6–100” means the size fraction 3–6 mm in the height of 100 mm. Fig. 4(b), 4(c) and 4(d) are the comparisons of empirical probability and calculated probability in three heights of pile. The results indicated the empirical probability and calculated probability of each size fraction were almost equal in three heights, which demonstrated the surface probability model for the conveyor belt is feasible in single size fraction, but the differences between these two probabilities increased with the increase of size fraction, because the range of larger size fraction is bigger and the pile surface of larger size fraction is more rugged; In addition, the probability of every size fraction reduced with the increase of height.

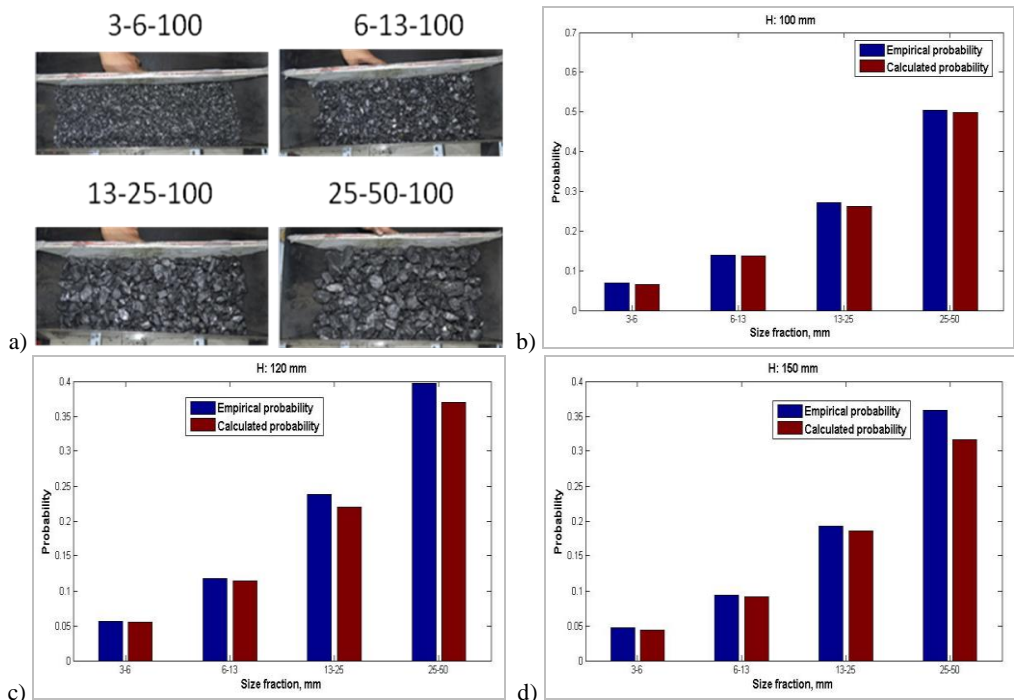


Fig. 4. (a): Images of four size fractions captured in the height of 100mm; (b), (c) and (d): Comparisons of empirical probability and calculated probability in three heights of pile

**Test two:** multiple size fractions were mixed to test the model in three heights (100 mm, 120 mm and 150 mm).

In order to recognize the size fractions of particles on the surface, particles of different size fractions were painted with different colors. Size fraction 3–6 mm is yellow and has 58500 particles; 6–13mm is red and has 9600 particles; 13–25 mm is blue and has 620 particles; 25–50 mm is self-colored and has 70 particles. Fig. 5(a) shows the number of particles in four size fractions. Multiple size fractions 3–13 mm, 3–25 mm and 3–50 mm were mixed respectively and used to compare the empirical probability and calculated probability of each size fraction in three heights of pile. Fig. 5(b), 5(c) and 5(d) shows multiple size fractions 3–13 mm, 3–25 mm and 3–50 mm in the height of 100 mm. The breadths (B) corresponding to heights 100 mm, 120 mm and 150 mm also were 434 mm, 476 mm and 532 mm, respectively. Dm of 3–13 mm, 3–25 mm and 3–50 mm were 5.205 mm, 5.334 mm and 5.367 mm, respectively. In each multiple size fraction, empirical probability and calculated probability of every

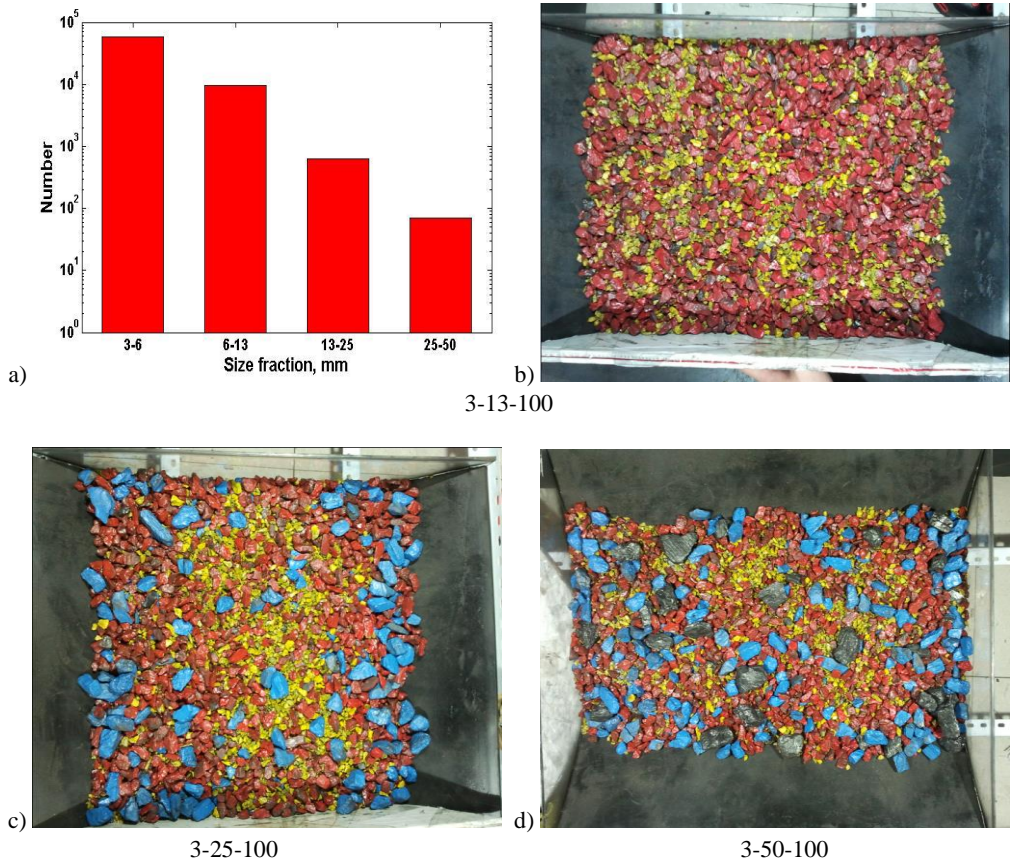
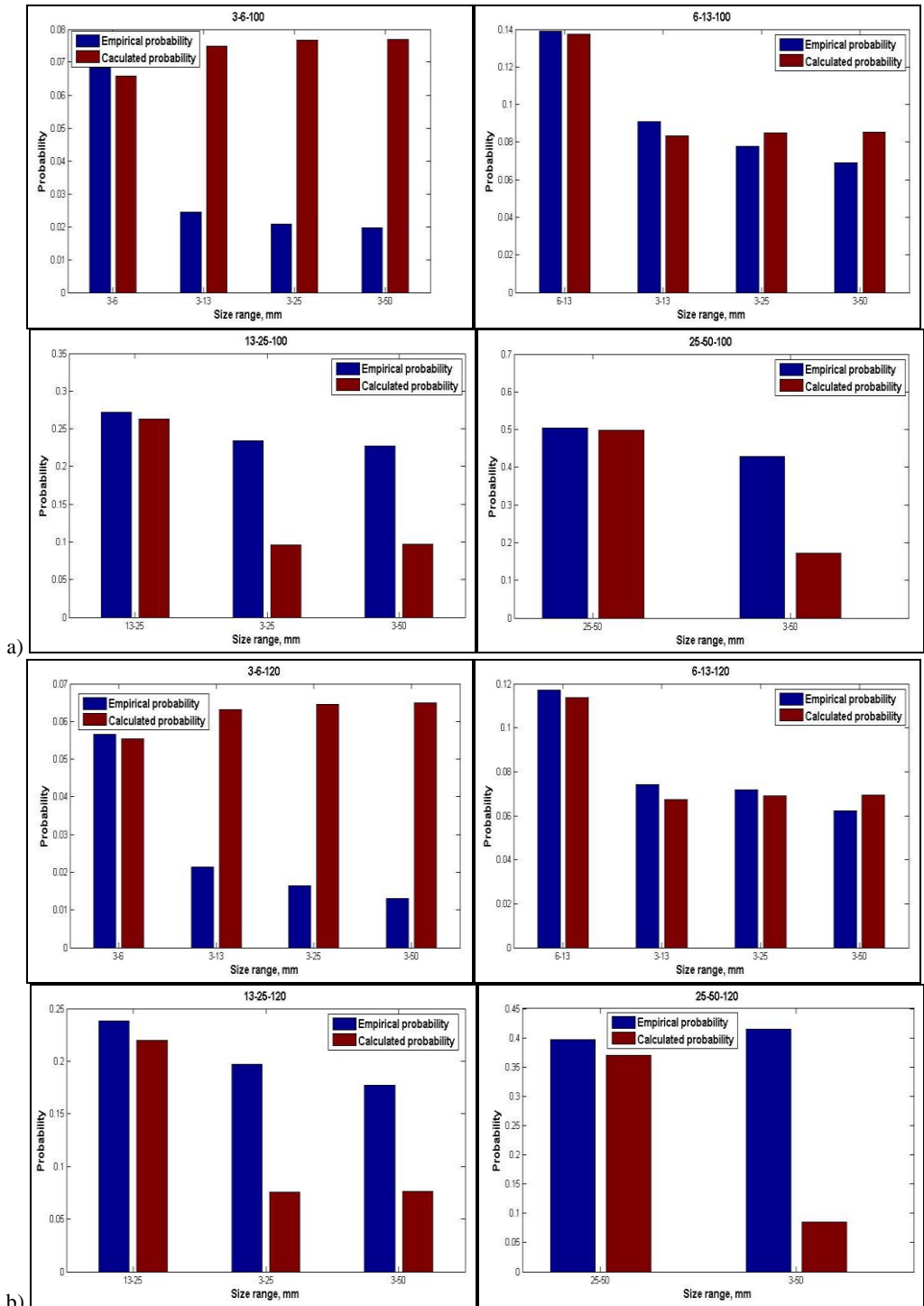


Fig. 5. (a): number of particles in four size fractions; (b), (c) and (d): multiple size



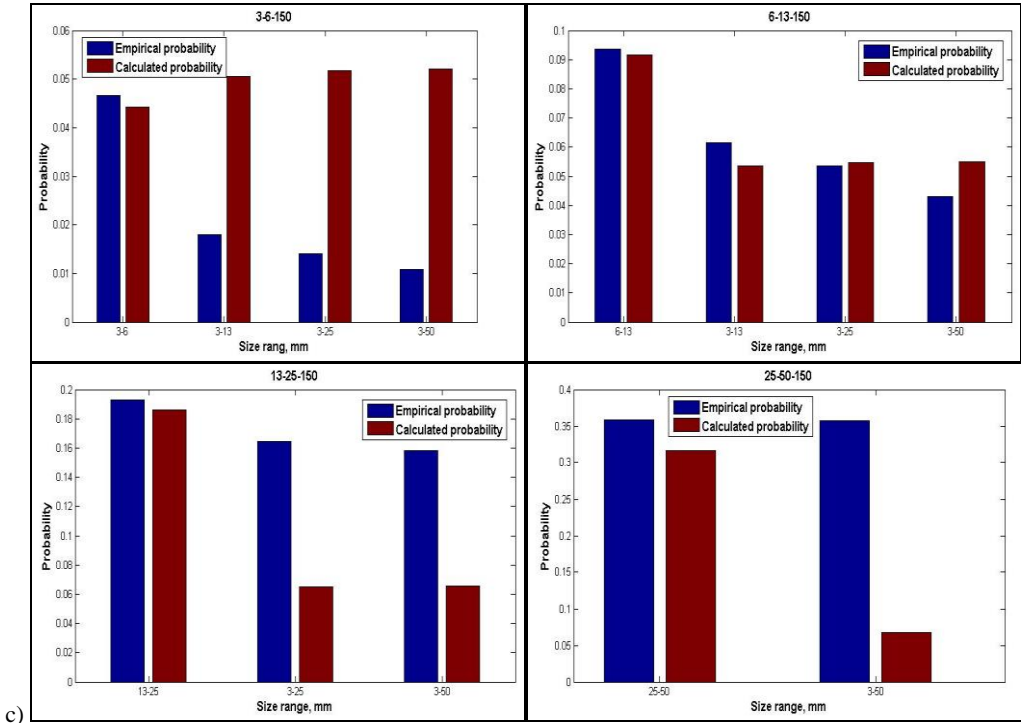


Fig. 6. Comparisons of empirical probability and calculated probability of every size fraction in multiple size fractions and different heights

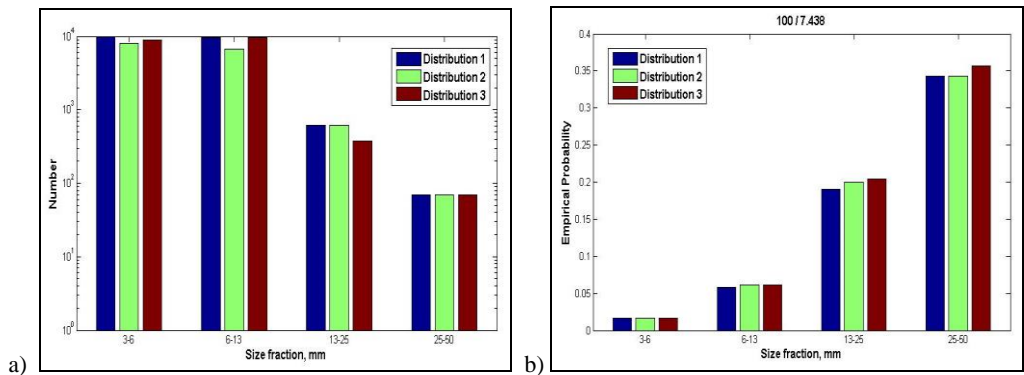
size fraction in different heights were obtained and showed in Fig. 6, which combined the results in test one. Results indicated the differences between empirical probability and calculated probability of each size fraction increased with the increase of range of multiple size fractions, the main reason of which is the covering of particles in different size fractions. In addition, empirical probabilities of 3–6 mm was smaller than calculated probabilities all the time; empirical probabilities of 6–13 mm was sometimes larger and sometimes smaller than calculated probabilities; empirical probabilities of 13–25 mm and 25–50 mm were larger than calculated probabilities all the time, which indicated larger particles should be easier to appear on the surface than smaller particles in multiple size fractions. Through comparisons in different heights, the higher the pile height is; the lower the difference between empirical probability and calculated probability is.

### Correction method for model error

Test one and test two indicated empirical probability and calculated probability of each size fraction were almost equal in single size fraction, but they were so different in multiple size fractions. The main reason is the covering of particles in different size

fractions. We considered the empirical surface probability as the “actual surface probability”, therefore, the difference between empirical and calculated probability is the error of surface probability model for conveyor belt. In engineering applications, piles usually had wide range of multiple size fractions. Therefore, particles of 3-50mm were used to find the relationship between empirical and calculated probability and try to propose a method to correct the model error.

According to a constant size range of particles, only the size distribution and the height of pile in belt were the variables.  $Dm$  can stand for the condition of size distribution of number in a degree. However, different size distributions maybe have the same value of  $Dm$ , and the empirical probability of every size fraction maybe change, but the calculated probability is constant in a constant height of pile. In this condition, a pile with three different size distributions (shown in Fig. 7(a)) but with the same value of  $Dm$  ( $Dm = 7.438$ ) was used to investigate the changes of empirical probability in three heights, the results of which were shown in Fig. 7(b), 7(c) and 7(d). In expression “100/7.438”, “100” means the height of pile and “7.438” means the value of  $Dm$ . Results indicated the empirical probabilities of every size fraction in three different size distributions were almost equal in three heights of pile. Therefore, we can consider one  $Dm$  corresponds to one empirical probability in a constant height of pile, in spite of the change of size distributions. One  $Dm$  also corresponds to one calculated probability in a constant height of pile, therefore, variation tendencies of empirical probability and calculated probability with  $Dm$  can be obtained to find some relationships.



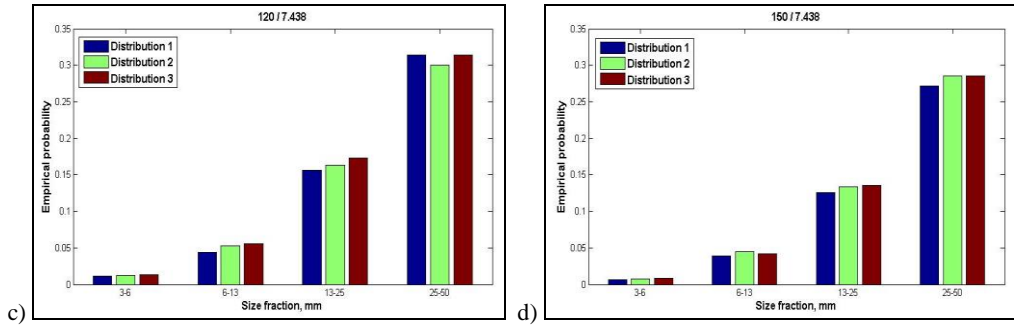


Fig. 7. (a): three different size distributions with the same value of  $D_m$ ; (b), (c) and (d): comparisons of empirical probabilities of four size fractions in three size distributions and three heights of pile

Finally, three heights (100 mm, 120 mm and 150 mm) of piles and five different  $D_m$  (5.367 mm, 6.037 mm, 7.438 mm, 8.399 mm and 9.7799 mm) were used to find the relationship between empirical and calculated probability. Fig. 8(a) shows the particle numbers of four size fractions corresponding to five different  $D_m$ . These four size fractions were the colored particles on test two. Because particles in 3–6mm were much more than other size fractions, only adjusting the number of particles in 3–6 mm will obtain five different  $D_m$  easily. We defined the correction factor ( $r$ ) as Eq. (8).

$$r = \frac{\text{Empirical probability}}{\text{Calculated probability}} \tag{8}$$

Fig. 8(b), 8(c) and 8(d) showed the variation tendencies of empirical probability, calculated probability and the correction factor with  $D_m$  in three heights of pile. The Y-axis of every trend image used LOG coordinate for the convenience of data display. Results indicated the variation tendencies of empirical probability and calculated probability with  $D_m$  were not the same in four size fractions, but the correction factor of four size fractions reduced with the increase of  $D_m$  in three heights. We used linear equation to model the correction factor and  $D_m$  by software MATLAB, showing in Fig. 8(a), 8(b) and 8(c). R-square and Root-Mean-Square Error (RMSE) were used to measure the goodness of fitting of linear equations, which indicated these equations were well fitted. Twelve fitting equations were as follows:

$$3-6-100: \quad r = -0.035 D_m + 0.4286 \tag{9}$$

$$3-6-120: \quad r = -0.02669 D_m + 0.3354 \tag{10}$$

$$3-6-150: \quad r = -0.03197 D_m + 0.3594 \tag{11}$$

$$6-13-100: \quad r = -0.1037 D_m + 1.322 \tag{12}$$

$$6-13-120: \quad r = -0.1156 D_m + 1.445 \tag{13}$$

$$6-13-150: \quad r = -0.129 Dm + 1.494 \quad (14)$$

$$13-25-100: \quad r = -0.3214 Dm + 3.989 \quad (15)$$

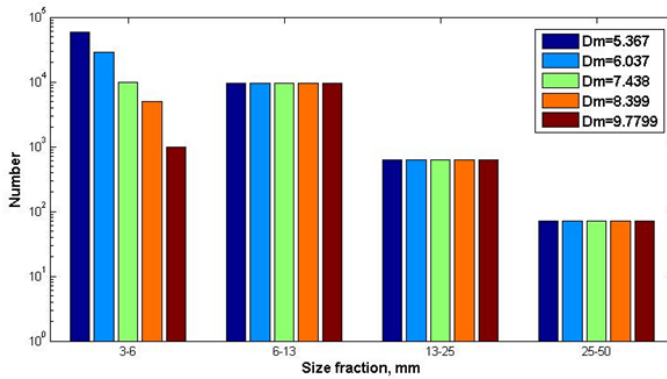
$$13-25-120: \quad r = -0.2869 Dm + 3.782 \quad (16)$$

$$13-25-150: \quad r = -0.3346 Dm + 4.07 \quad (17)$$

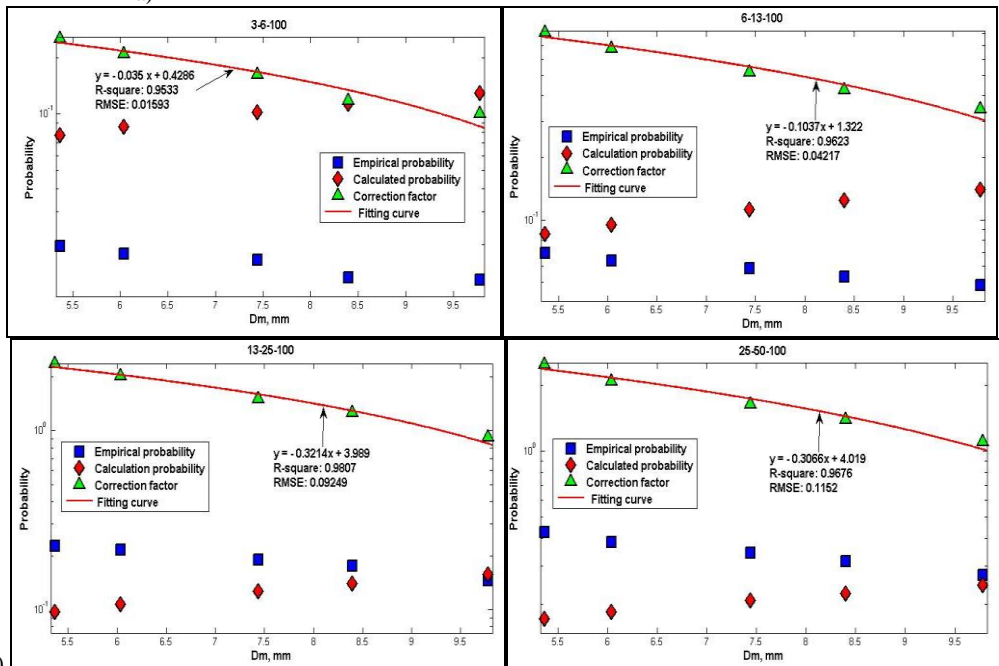
$$25-50-100: \quad r = -0.3066 Dm + 4.019 \quad (18)$$

$$25-50-120: \quad r = -0.6866 Dm + 8.147 \quad (19)$$

$$25-50-150: \quad r = -0.8358 Dm + 9.546 \quad (20)$$



a)



b)

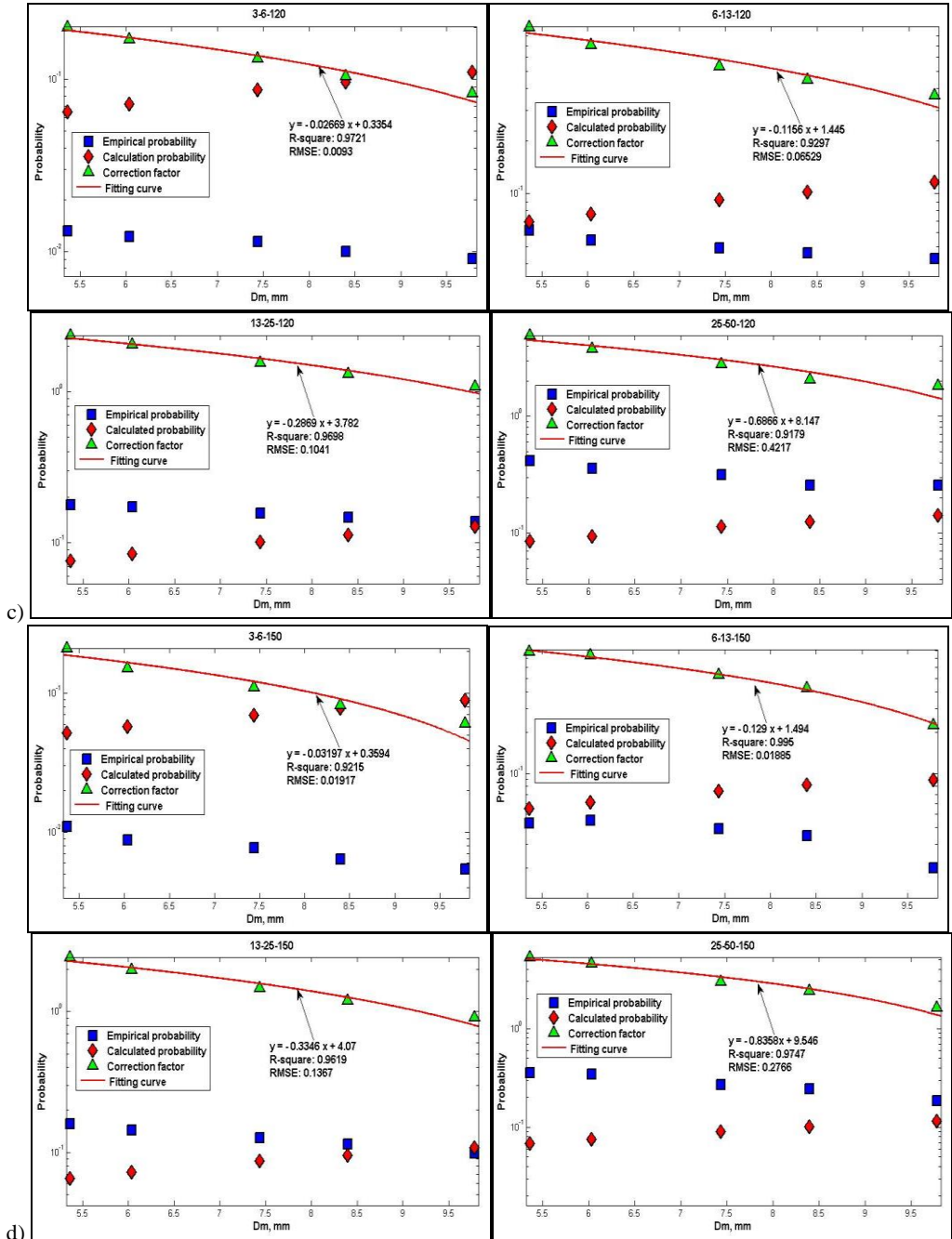


Fig. 8. (a): size distributions corresponding to five different values of Dm; (b), (c) and (d): variation tendencies of empirical probability, calculated probability and the correction factor of four size fractions with Dm in three heights of pile

These linear equations showed different size fractions and heights of pile had different correction model. Therefore, according to  $Dm$  and the height of particle pile of 3–50 mm, a corresponding correction equation can be selected to calculate the correction factor and correct the error of surface probability model. More correction equations in different conditions needed to be developed in the future.

## Conclusions

A new surface probability model for the estimation of particles size distribution on a conveyor belt was developed based on Chavez model, which can be used to correct the capturing error and improve the estimation accuracy of size distribution by image analysis in mineral engineering. A series of experiments were carried out to test and verify the new model and several conclusions were obtained as follows:

- The empirical probability and calculated probability of each size fraction were almost equal in single size fraction, and the two probabilities of each size fraction reduced with the increase of height of pile.
- Differences between empirical probability and calculated probability of each size fraction increased with the increase of range of multiple size fractions, the main reason of which is the covering of particles in different size fractions. In addition, larger particles should be easier to appear on the surface than smaller particles in multiple size fractions. In addition, the higher the pile height is, the lower the difference between empirical probability and calculated probability is.
- One  $Dm$  corresponds to one empirical probability in a constant height of pile, in spite of the change of size distributions.
- The variation tendencies of empirical probability and calculated probability with  $Dm$  were not the same in four size fractions, but the correction factor of four size fractions reduced with the increase of  $Dm$  in three heights.
- A series of linear equations of correction factor and  $Dm$  were developed to correct the errors between empirical probability and calculated probability, and more correction equations in different conditions needed to be developed in the future

## Acknowledgements

The authors would like to thank the National Natural Science Foundation of China (No.51304192), Specialized Research Fund for the Doctoral Program of Higher Education (No. 20130095110005) and Colleges and Universities in Jiangsu Province plans to graduate research and innovation (CXZZ13\_0951).

## References

- Al-Thyabat S., Miles N.J., 2006. *An improved estimation of size distribution from particle profile measurements*. Powder Technology 166, 152–160.
- Al-Thyabat S., Miles N.J., Koh T.S., 2007. *Estimation of the size distribution of particles moving on a conveyor belt*. Minerals Engineering 20, 72–83.
- Casali A., Gonzalez G., Vallebuona G., Perez C., Vargas R., 2001. *Grindability Softsensors based on Lithological Composition and On-Line Measurements*. Minerals Engineering 14, 689–700.

- Chavez R., Cheimanoff N., Schleifer J., 1996. *Sampling problems during grain size distribution measurements*. In: Proceedings of the Fifth International Symposium on Rock Fragmentation by Blasting - FRAGBLAST 5. Montreal, Quebec, Canada, 245–252.
- Claudio A., Pablo A., Estévez A., 2011. *Ore grade estimation by feature selection and voting using boundary detection in digital image analysis*. International Journal of Mineral Processing 101, 28–36.
- Chatterjee S., Bandopadhyay S., Machuca D., 2010a. *Ore Grade Prediction Using a Genetic Algorithm and Clustering based Ensemble Neural Network Model*. Mathematical Geosciences 42, 309–326.
- Chatterjee S., Bhattacharjee A., Samanta B., Pal S.K., 2010b. *Image-based Quality Monitoring System of Limestone Ore Grades*. Computers in Industry 16, 391–408.
- Guyot O., Monredon T., LaRosa D., Broussaud A., 2004. *VisioRock, an Integrated Vision Technology for Advanced Control of Comminution Circuits*. Minerals Engineering 17, 1227–1235.
- Jayson T., Carl D., Gianni B., 2007. *A machine vision approach to on-line estimation of run-of-mine ore composition on conveyor belts*. Minerals Engineering 20, 1129–1144.
- Kemeny J., Mofya E., Kaunda R., Lever P., 2001. *Improvements in blast fragmentation models using digital image processing*, in: Explosives in Mining Conference, Explo, 357–363.
- King R.P., 1982. *Determination of the distribution of size of irregularly shaped particles from measurements on sections or projected areas*. Powder Technology 32, 87–100.
- Ko Y. D., Shang H., 2011. *Time delay neural network modeling for particle size in SAG mills*. Powder Technology 205, 250–262.
- Petruk W., 1988a. *Automatic image analysis for mineral beneficiation*. Journal of Metals 40 (4), 29–31.
- Petruk W., 1988b. *Automatic image analysis to determine mineral behaviour during mineral beneficiation*, Process Mineralogy VIII. In: Carson, D.J.T., Vassiliou, A.H. (Eds.). The Minerals, Metals & Materials Society, 347–357.
- Petruk W., 1989, *Short course on image analysis applied to mineral and earth sciences*, Mineralogical Association of Canada, Ottawa.
- Petruk W., Wilson J.M.D., Lastra R., Healy R.E., 1991. *An image analysis and materials balancing procedure for evaluating ores and mill products to obtain optimum recoveries*. In: Proceedings of 23rd Annual Meeting of the Canadian Mineral Processors, 1–16 (Section 19).
- Perez C., Casali A., Gonzalez G., Vallebuona G., Vargas R., 1999. *Lithological Composition Sensor based on Digital Image Feature Extraction, Genetic Selection of Features and Neural Classification*. IEEE International Conference on Information Intelligence and Systems, Bethesda, MD, Oct.31–Nov.3, 236–241.
- Singh V., Rao S., 2006. *Application of Image Processing in Mineral Industry: a Case Study of Ferruginous Manganese Ores*. Mineral Processing and Extractive Metallurgy 115, 155–160.
- Singh N., Singh T. N., Tiwary A., Sarkar K.M., 2010. *Textural identification of basaltic rock mass using image processing and neural network*. Computers & Geosciences 14, 301–310.
- Sun J., Su B., 2013. *Coal-rock interface detection on the basis of image texture features*. International Journal of Mining Science and Technology 23, 681–687.
- Tessier J., Duchesne C., Bartolacci G., 2007. *A Machine Vision Approach to On-line Estimation of Run-of-mine Ore Composition on Conveyor Belts*. Minerals Engineering 20, 1129–1144.
- Vallebuona G., Arbuo K., Casali A., 2003. *A procedure to estimate weight particle distributions from area measurements*. Minerals Engineering 16, 323–329.
- Yang H., Liu Y., Xie H., Xu Y., Sun Q., Wang, S., 2013. *Integrative method in lithofacies characteristics and 3D velocity volume of the Permian igneous rocks in H area, Tarim Basin*. International Journal of Mining Science and Technology 23, 167–172.

Zhao Y., 2013. *Multi-level denoising and enhancement method based on wavelet transform for mine monitoring*. International Journal of Mining Science and Technology 23, 163–166.

Zhang Z., Yang J., Ding L., Zhao Y.M., 2012. *An improved estimation of coal particle mass using image analysis*. Powder Technology 229, 178–184.